Supporting Information

Facile Construction of Hollow In_2S_3/Polymeric Carbon Nitride Heterojunction for Efficient Visible-Light-Driven CO_2 Reduction

Shuangchao Zhao[a], Keyan Li[a,*], Jun Du[a], Chunshan Song[a,b], Xinwen Guo[a,*]

[a]*State Key Laboratory of Fine Chemicals, PSU-DUT Joint Center for Energy Research, School of Chemical Engineering, Dalian University of Technology, Dalian 116024, China.*

[b]*Department of Chemistry, Faculty of Science, The Chinese University of Hong Kong, Shatin, NT, Hong Kong, China*

**Corresponding Author. E-mail address: keyanli@dlut.edu.cn; guoxw@dlut.edu.cn.*

Number of pages: 9

Number of figures: 8

Number of tables: 3

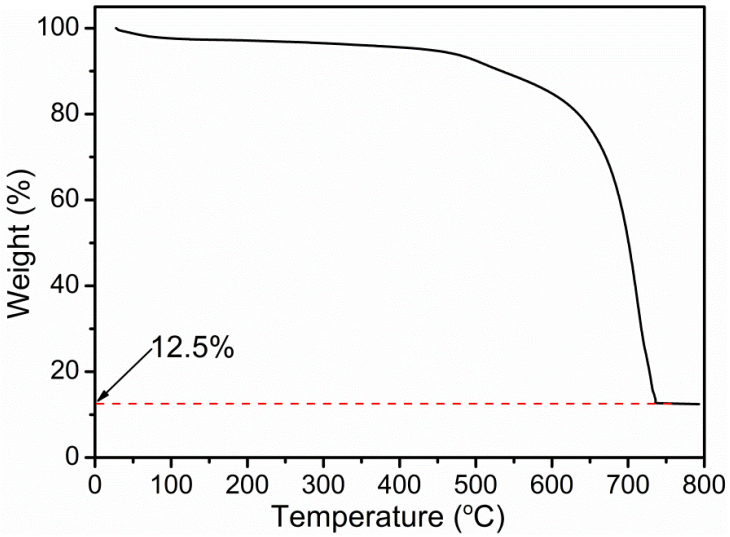

Figure S1. TG curve of IS/CN-5.

When IS/CN-5 is heated to 800 °C in air, CN is decomposed completely and In_2S_3 is transformed into In_2O_3. The content of In_2O_3 is 12.5%, and the content of In_2S_3 is calculated to be 14.7% according to the conservation of indium.

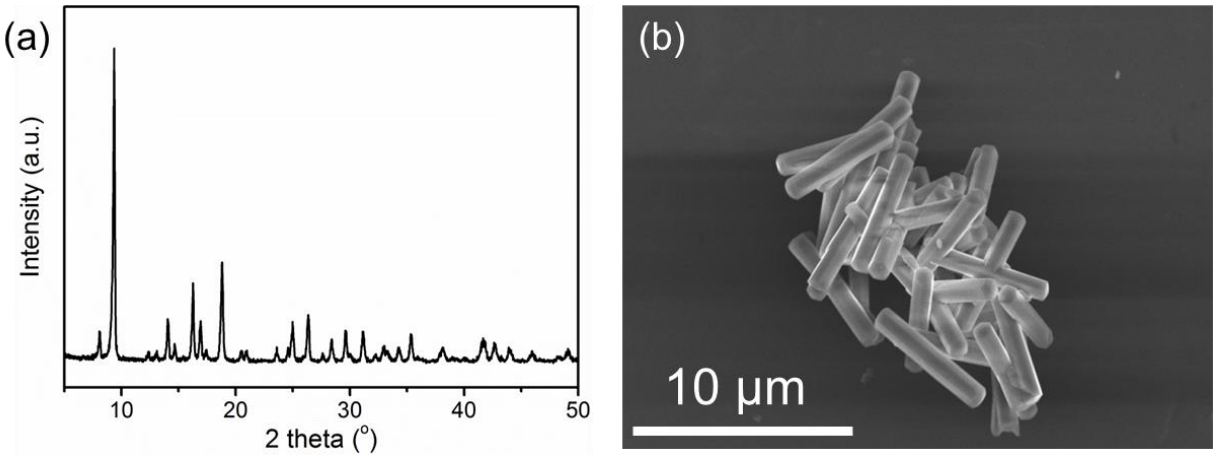

Figure S2. (a) XRD pattern and (b) SEM image of In-MIL-68.

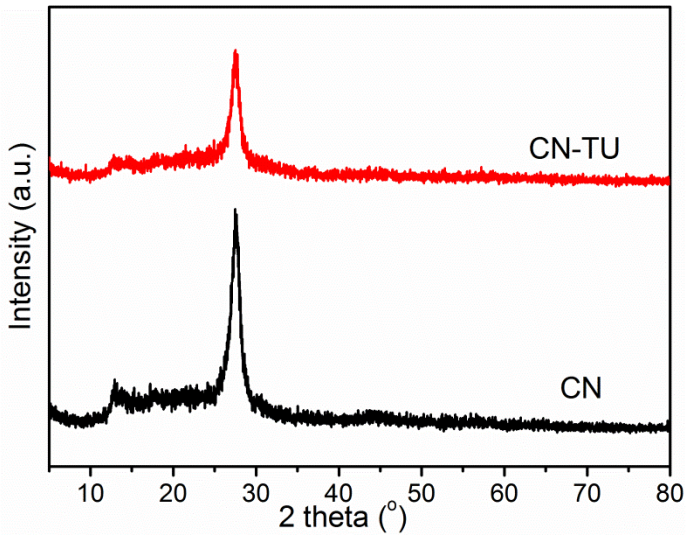

Figure S3. XRD patterns of CN and CN-TU.

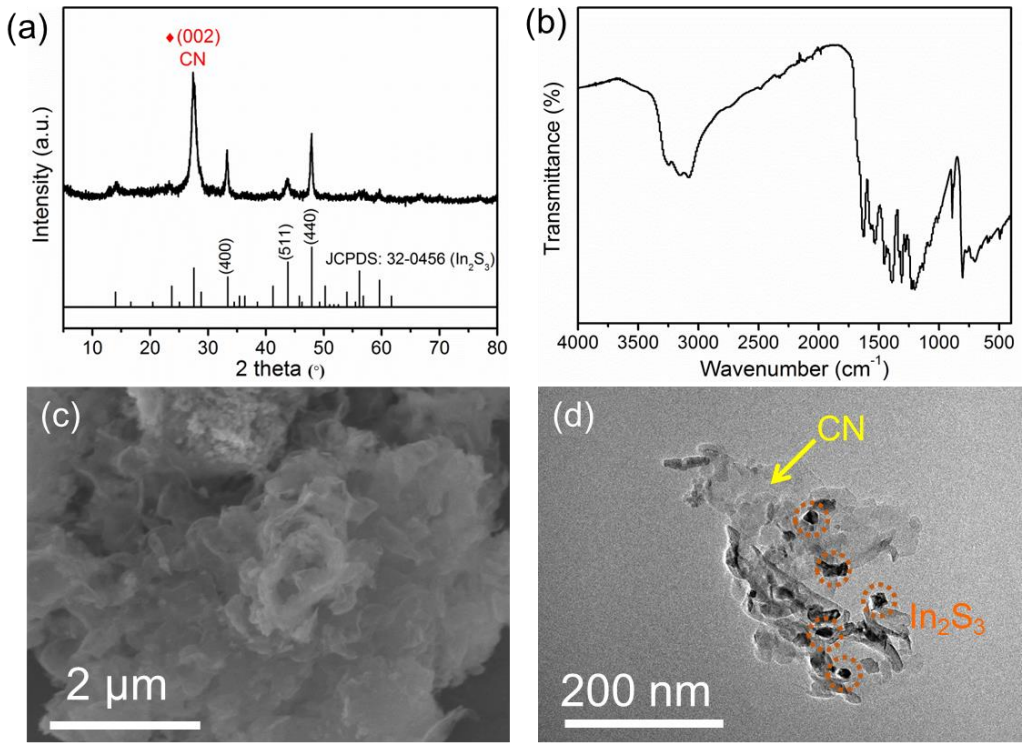

Figure S4. (a) XRD pattern, (b) FT-IR spectrum, (c) SEM image and (d) TEM image of IS-NP/CN.

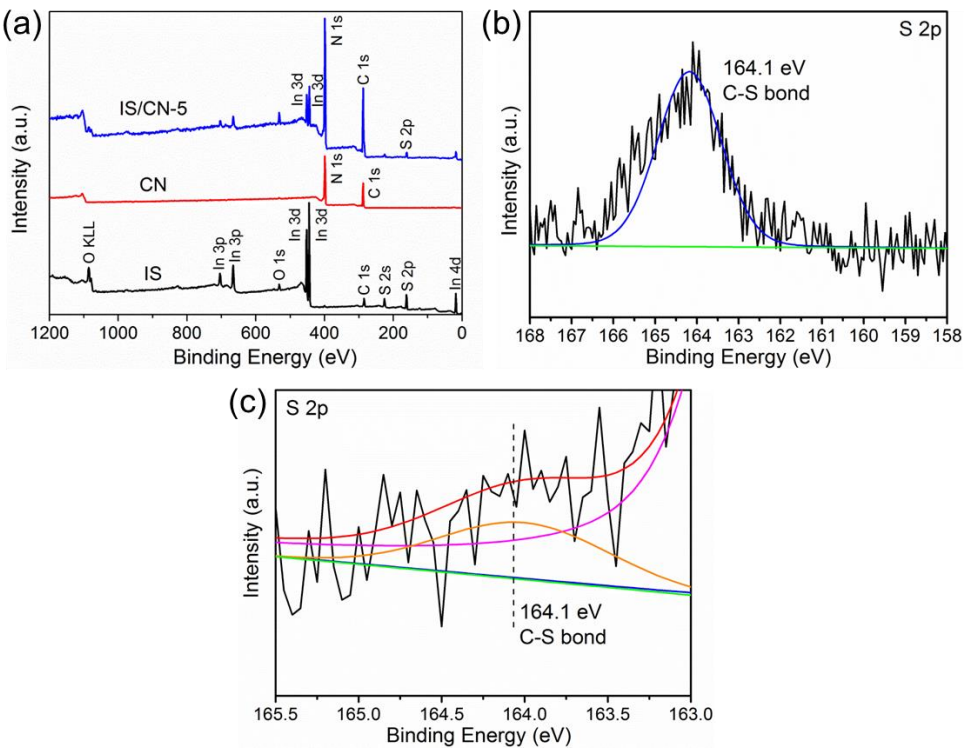

Figure S5. (a) XPS survey spectra of IS, CN and IS/CN-5, S 2p XPS spectra of (b) CN-TU and (c) IS/CN-5.

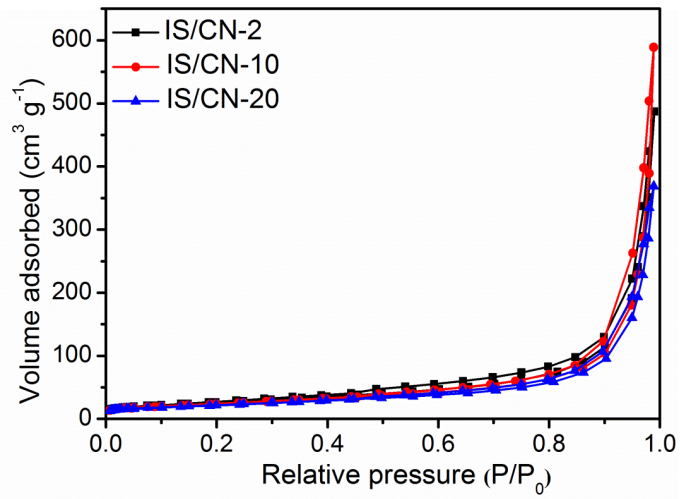

Figure S6. N_2 adsorption-desorption isotherms of IS/CN-2, IS/CN-10 and IS/CN-20.

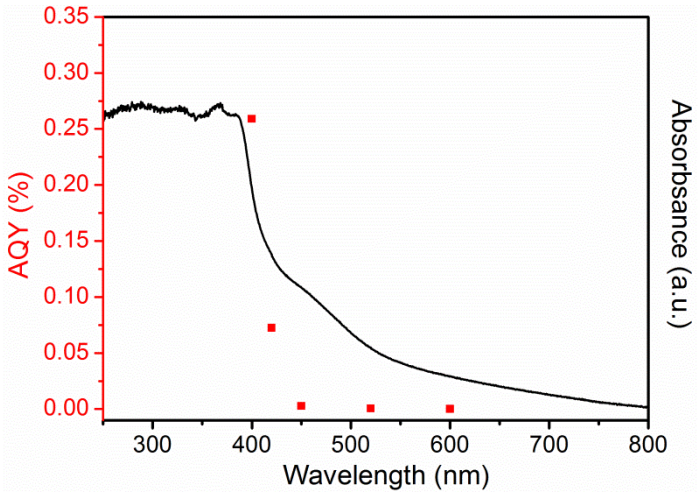

Figure S7. Wavelength dependent AQY of IS/CN-5.

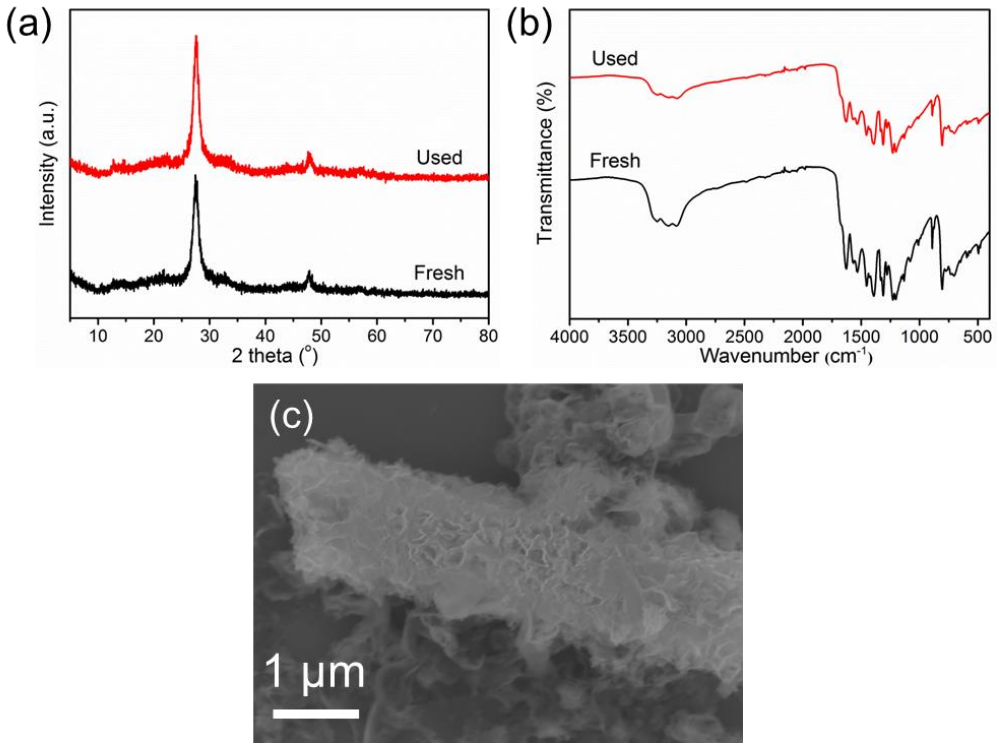

Figure S8. (a) XRD patterns and (b) FT-IR spectra of IS/CN-5 before and after reaction. (c) SEM image of IS/CN-5 after reaction.

Table S1. Zeta potentials of In-MIL-68 and CN.

Sample	Zeta potential (mV)
In-MIL-68	–8.53
CN	6.86

Table S2. BET surface area, CO and H_2 generation rates and the selectivity of CO of the as-prepared samples.

Sample	BET surface area ($m^2\ g^{-1}$)	CO generation rate ($\mu mol\ g^{-1}\ h^{-1}$)	H_2 generation rate ($\mu mol\ g^{-1}\ h^{-1}$)	CO selectivity (%)
IS	95	4.9	16.0	23.4
IS/CN-2	96	351.2	79.3	81.6
IS/CN-5	86	483.4	112.7	81.1
IS/CN-10	87	439.5	98.6	81.7
IS/CN-20	79	397.0	78.6	83.5
CN	112	80.6	19.2	80.8

Table S3. Comparison of the photocatalytic CO_2 conversion performance of IS/CN-5 with those of other photocatalysts reported in the literature.

Photocatalyst	Cocatalyst	Sacrificial agent	Main product generation rate (μmol g^{-1} h^{-1})	Ref.
CdS/BCN	$Co(bpy)_3^{2+}$	TEOA	CO: 250	1
Co_4@g-C_3N_4	$Co(bpy)_3^{2+}$	TEOA	CO: 114.4	2
UiO-66/CNNS	/	TEOA	CO: 9.9	3
HR-CN	$Co(bpy)_3^{2+}$	TEOA	CO: 296.7	4
Co_3O_4/2D g-C_3N_4	$Co(bpy)_3^{2+}$	TEOA	CO: 419	5
BCN-30	$Co(bpy)_3^{2+}$	TEOA	CO: 93	6
TiO_{2-x}/MCN	$Co(bpy)_3^{2+}$	TEOA	CO: 77.8	7
Co doped TiO_2/g-C_3N_4	$Co(bpy)_3^{2+}$	TEOA	CO: 287.4	8
In_2S_3-$CuInS_2$	$Co(bpy)_3^{2+}$	TEOA	CO: 19	9
$BiFeWO_x$@In_2S_3	/	TEOA	CO: 28.9 CH_4: 49.9	10
TCN(NH_3)	$Co(bpy)_3^{2+}$	TEOA	CO: 103.6	11
BIF-20@g-C_3N_4	/	TEOA	CO: 53.9 CH_4: 15.5	12
$ZnIn_2S_4$@CNO	$Co(bpy)_3^{2+}$	TEOA	CO: 253.8	13
g-C_3N_4/CdS	$Co(bpy)_3^{2+}$	TEOA	CO: 234.6	14
DA-CTF	$Co(bpy)_3^{2+}$	TEOA	CO: 155	15
IS/CN-5	$Co(bpy)_3^{2+}$	TEOA	CO: 483.4	This work

References

1. Zhou, M.; Wang, S.; Yang, P.; Huang, C.; Wang, X. Boron Carbon Nitride Semiconductors Decorated with CdS Nanoparticles for Photocatalytic Reduction of CO_2. *ACS Catal.* **2018,** *8*, 4928-4936.

2. Zhou, J.; Chen, W.; Sun, C.; Han, L.; Qin, C.; Chen, M.; Wang, X.; Wang, E.; Su, Z. Oxidative Polyoxometalates Modified Graphitic Carbon Nitride for Visible-Light CO_2 Reduction. *ACS Appl. Mater. Interfaces* **2017,** *9*, 11689-11695.

3. Shi, L.; Wang, T.; Zhang, H.; Chang, K.; Ye, J. Electrostatic Self-Assembly of Nanosized Carbon Nitride Nanosheet onto a Zirconium Metal-Organic Framework for Enhanced Photocatalytic CO_2 Reduction. *Adv. Funct. Mater.* **2015,** *25*, 5360-5367.

4. Zheng, Y.; Lin, L.; Ye, X.; Guo, F.; Wang, X. Helical Graphitic Carbon Nitrides with Photocatalytic and Optical Activities. *Angew. Chem., Int. Ed.* **2014,** *53*, 11926-11930.

5. Zhu, X.; Ji, H.; Yi, J.; Yang, J.; She, X.; Ding, P.; Li, L.; Deng, J.; Qian, J.; Xu, H.; Li, H. A Specifically Exposed Cobalt Oxide/Carbon Nitride 2D Heterostructure for Carbon Dioxide Photoreduction. *Ind. Eng. Chem. Res.* **2018,** *57*, 17394-17400.

6. Huang, C.; Chen, C.; Zhang, M.; Lin, L.; Ye, X.; Lin, S.; Antonietti, M.; Wang, X. Carbon-Doped BN Nanosheets for Metal-Free Photoredox Catalysis. *Nat. Commun.* **2015,** *6*, 7698-7705.

7. Shi, H.; Long, S.; Hu, S.; Hou, J.; Ni, W.; Song, C.; Li, K.; Gurzadyan, G. G.; Guo, X. Interfacial Charge Transfer in 0D/2D Defect-Rich Heterostructures for Efficient Solar-Driven CO_2 Reduction. *Appl. Catal., B* **2019,** *245*, 760-769.

8. Shi, H.; Du, J.; Hou, J.; Ni, W.; Song, C.; Li, K.; Gurzadyan, G. G.; Guo, X. Solar-Driven CO_2 Conversion over Co^{2+} Doped 0D/2D TiO_2/g-C_3N_4 Heterostructure: Insights into the Role of Co^{2+}

and Cocatalyst. *J. CO_2 Util.* **2020,** *38*, 16-23.

9. Yang, J.; Zhu, X.; Mo, Z.; Yi, J.; Yan, J.; Deng, J.; Xu, Y.; She, Y.; Qian, J.; Xu, H.; Li, H. A Multidimensional In_2S_3-$CuInS_2$ Heterostructure for Photocatalytic Carbon Dioxide Reduction. *Inorg. Chem. Front.* **2018,** *5*, 3163-3169.

10. Wang, Y.; Zeng, Y.; Wan, S.; Zhang, S.; Zhong, Q. Construction of Octahedral $BiFeWO_x$ Encapsulated in Hierarchical In_2S_3 Core@Shell Heterostructure for Visible-Light-Driven CO_2 Reduction. *J. CO_2 Util.* **2019,** *29*, 156-162.

11. Mo, Z.; Zhu, X.; Jiang, Z.; Song, Y.; Liu, D.; Li, H.; Yang, X.; She, Y.; Lei, Y.; Yuan, S.; Li, H.; Song, L.; Yan, Q.; Xu, H. Porous Nitrogen-Rich g-C_3N_4 Nanotubes for Efficient Photocatalytic CO_2 Reduction. *Appl. Catal., B* **2019,** *256*, 117854.

12. Xu, G.; Zhang, H.; Wei, J.; Zhang, H. X.; Wu, X.; Li, Y.; Li, C.; Zhang, J.; Ye, J. Integrating the g-C_3N_4 Nanosheet with B-H Bonding Decorated Metal-Organic Framework for CO_2 Activation and Photoreduction. *ACS Nano* **2018,** *12*, 5333-5340.

13. Zhu, K.; Ou-Yang, J.; Zeng, Q.; Meng, S.; Teng, W.; Song, Y.; Tang, S.; Cui, Y. Fabrication of Hierarchical $ZnIn_2S_4$@CNO Nanosheets for Photocatalytic Hydrogen Production and CO_2 Photoreduction. *Chin. J. Catal.* **2020,** *41*, 454-463.

14. Vu, N.-N.; Kaliaguine, S.; Do, T.-O. Synthesis of the g-C_3N_4/CdS Nanocomposite with a Chemically Bonded Interface for Enhanced Sunlight-Driven CO_2 Photoreduction. *ACS Appl. Energy Mater.* **2020,** *3*, 6422-6433.

15. Zhong, H.; Hong, Z.; Yang, C.; Li, L.; Xu, Y.; Wang, X.; Wang, R. A Covalent Triazine-Based Framework Consisting of Donor-Acceptor Dyads for Visible-Light-Driven Photocatalytic CO_2 Reduction. *ChemSusChem* **2019,** *12*, 4493-4499.